Available online at www.sciencedirect.com
SCIENCE @ DIRECT®

Thin Solid Films 438–439 (2003) 457–461

www.elsevier.com/locate/tsf

Wiring up single molecules

Jiwoong Park[a,c], Abhay N. Pasupathy[a], Jonas I. Goldsmith[b], Alexander V. Soldatov[d], Connie Chang[a], Yuval Yaish[a], James P. Sethna[a], Héctor D. Abruña[b], Daniel C. Ralph[a], Paul L. McEuen[a,*]

[a]Laboratory of Atomic and Solid State Physics, Cornell University, Ithaca, NY 14853, USA
[b]Department of Chemistry and Chemical Biology, Cornell University, Ithaca, NY 14853, USA
[c]Department of Physics, University of California, Berkeley, CA 94720, USA
[d]Department of Physics, Harvard University, Cambridge, MA 02138, USA

Abstract

The possibility of using single molecules as active elements of electronic devices offers a variety of scientific and technological opportunities. In this article, we discuss transistors, where electrons flow through discrete quantum states of a single molecule. First, we will describe molecules, where current flows through one cobalt atom surrounded by two insulating terpyridyl ligands. Depending on the length of the insulating part of the molecules, two different behaviors are observed: Coulomb blockade for a longer molecule and the Kondo effect for a shorter molecule. We will also discuss measurements of the C_{70} fullerene and its dimer (C_{140}). In C_{140} devices, the transport measurements are affected by an intercage vibrational mode that has an energy of 11 meV. We observe a large current increase when this mode is excited, indicating a strong coupling between the electronic and mechanical degrees of freedom in C_{140} molecules.

Keywords: Molecular electronics; Nanostructures; Electrical properties; Measurements

1. Introduction

Understanding electron transport phenomena in a single molecule regime will offer a new way for approaching many interesting and fundamental problems in nanometer-scale physics [1]. Several recent experiments have investigated electron transport in single molecules. In most of the cases, the biggest experimental challenge is to develop a technique to reproducibly 'wire up' a single molecule. Scanning probe microscopy techniques with STM or AFM have been widely used successfully to measure the conductance of molecules in the single-molecule limit [2,3]. Mechanical break junctions have also been used in several groundbreaking experiments [4,5]. More recently, other approaches have been developed to fabricate electrodes spaced by an nm-scale gap sufficiently small to wire up molecules in a planar geometry. The electromigration-junction technique, which we use was originally developed by H. Park et al. [6,7]. Using the electromigration technique, we have succeeded in wiring up single molecules in which current flow occurs via tunneling through a single cobalt atom [8]. In this article, we will discuss the results from these molecules along with additional measurements on two different fullerene molecules.

2. Experimental

The molecules that we have investigated are depicted in Fig. 1a. Molecules I and II are coordination complexes in which one Co ion is bonded to two terpyridyl linker molecules with thiol end groups, which confer high adsorbability onto gold surfaces. The two molecules differ by a 5-carbon alkyl chain within the linker molecules. It is known from electrochemical studies that the charge state of these molecules can be changed from 2+ to 3+ at low energy [9]. The other two molecules studied in this experiment are the fullerene C_{70} and its dimer C_{140} (molecules III and IV). C_{70} powder was obtained commercially and used without further purification. C_{140} was synthesized and purified by the method described in S. Lebedkin et al. [10].

The fabrication of single molecule transistors begins by defining a gate region on a silicon wafer. For molecules I and II, the substrate of degenerately doped

---

*Corresponding author. Tel.: +1-607-255-4176.
E-mail address: mceuen@ccmr.cornell.edu (P.L. McEuen).

0040-6090/03/$ - see front matter © 2003 Elsevier Science B.V. All rights reserved.
doi:10.1016/S0040-6090(03)00805-8

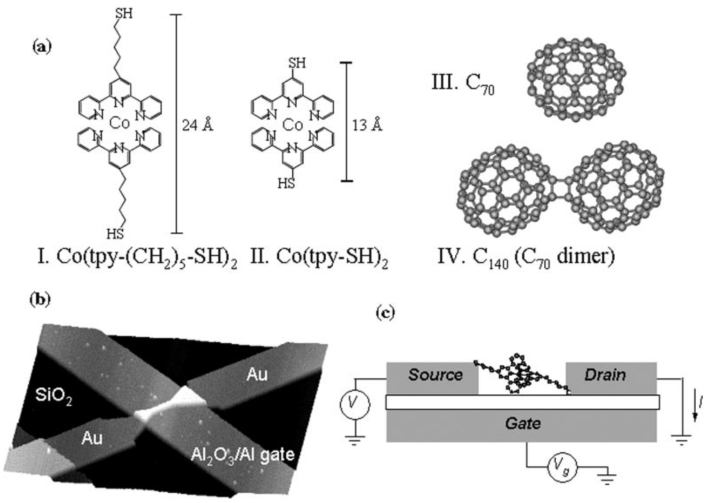

Fig. 1. (a) The molecules used in this study. (b) A topographic AFM image (5×5 μm) of a gold wire fabricated on top of an Al/Al_2O_3 gate electrode. This geometry was used to study the molecule III and IV. (c) The schematic diagram of a device with the measurement setup is shown.

silicon with 30 nm thick thermal oxide is used for a back gate. For fullerene molecules III and IV, an aluminium gate with 1–2 nm native oxide is lithographically defined on a silicon oxide surface. Then continuous gold nanowires with a width less than 200 nm, a length of approximately 200 nm and a thickness of approximately 30 nm are fabricated on top of the gate region by electron beam lithography and lift-off (see Fig. 1b). These wires are carefully cleaned with acetone, methylene chloride and oxygen plasma, after which the molecules are deposited by placing the wires in a dilute solution to form a self-assembled monolayer (molecules I and II) or by a direct deposition of the solution and a nitrogen blow dry (molecules III and IV).

The wires are cooled to liquid helium temperatures or below, before the electromigration process is begun. Using electromigration, the wires are broken to form an approximately 1 nm gap between two electrodes, a gap that can be bridged by single molecules [6]. Then the conductance of the device is measured at low biases as a function of the bias voltage (V) and gate voltage (V_g) to determine if any molecules have been incorporated across the gap. Molecules are found in less than 10% of the electrodes, which suggests that it is unlikely to have multiple molecules across one gap. The schematic of the finished device with the measurement setup is shown in Fig. 1c.

3. Results and discussion

3.1. Coulomb blockade in single molecule transistors (molecule I)

We begin with measurements from the long Co(tpy-$(CH_2)_5$-SH)$_2$ molecule (molecule I). Fig. 2a shows I–V curves measured in a device with the molecule I at different gate voltages. Each I–V curve displays a non-conducting region near zero bias whose width can be controlled by changing the gate voltage. This behavior can be well understood using the standard single electron transistor (SET) theory [11]. Tunneling of an additional electron on and off the molecule I is not allowed until tunneling electrons have enough energy to overcome the charging energy of the molecule, resulting in a non-conducting region near zero bias (Coulomb blockade). Therefore, the charge state of a molecule is fixed within the Coulomb blockade. By changing the gate voltage, the Coulomb blockade can be narrowed (widened) when the charge state of the molecule becomes less (more) stable.

Further analysis can be performed using a differential conductance (dI/dV) plot as shown in Fig. 2b. There are two triangular Coulomb blockade regions which meet at a gate voltage V_c. Previous electrochemical studies suggest that the charge state of the cobalt atom within the blockade region is 3+ (2+) for $V_g < V_c$ ($V_g > V_c$).

The blockade regions are bordered by bright dI/dV lines that correspond to the first current steps in I–V curves. According to the SET theory, these lines are due to electron tunneling through the quantum ground states of the molecule in either charge state at low biases. In this device, current flows by electrons tunneling on and off the molecule I while changing the charge state of the cobalt ion between 2+ and 3+. There are also additional lines outside the boundary and they correspond to quantum excitations of the molecule. A dI/dV line that meets the blockade region at $V_g < V_c$ ($V_g > V_c$) corresponds to an excited level of the molecule I in 3+

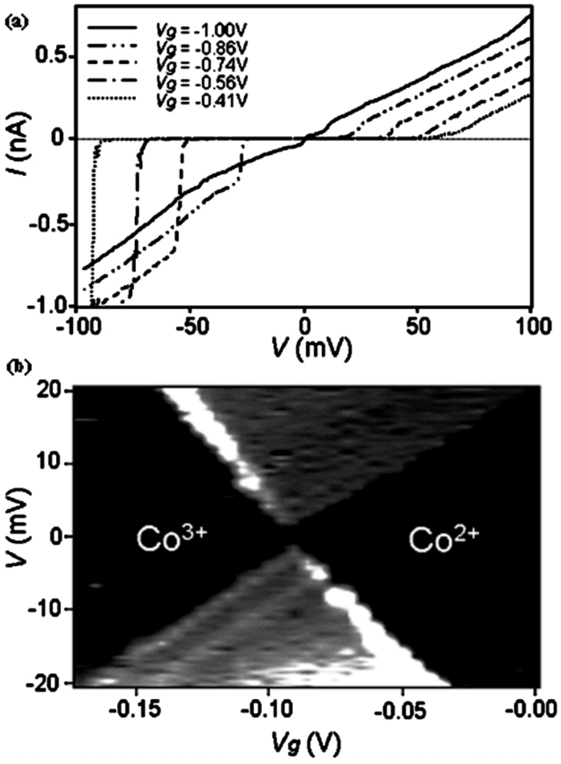

Fig. 2. Coulomb blockade in single molecule transistors (molecule I). (a) I–V curves measured at different gate voltages (V_g) from a device with molecule I. (b) A differential conductance (dI/dV) plot as a function of V and V_g measured at 1.5 K from a device with molecule I. The dI/dV increases from zero (black) to maximum (white). The charge state of the cobalt atom within the blockade region is 3+ or 2+ as shown in this figure.

(2+) charge state. The energy of the excitation can be measured from the bias voltage of the point where the line intercepts the Coulomb blockade.

Most devices with the SET behavior showed several excited levels at low biases (<6 meV). In these devices, we observed the same structure in excited levels for both charge states (not shown), which suggest that these low energy excitations are most likely vibrational [7]. Normal mode calculations done using a quantum chemistry package (HyperChem 7.0) indicate that there are more than 10 normal modes of this molecule within the same energy range.

Finally, the spin state of the molecule I was also studied. Upon applying magnetic fields, a device with the molecule I showed Zeeman splitting of the ground state for the 2+ charge state and a g-factor close to 2 (not shown). The 3+ charge state did not show any Zeeman splitting. This observation indicates that the 3+ state has spin 0. Further analysis using the magnitude of current at different magnetic fields confirmed that the cobalt atom has spin 1/2 for the +2 charge state and spin 0 for +3 charge state, in accord with previous chemical studies [12].

3.2. The Kondo effect in single molecule transistors (molecule II)

Unlike the transistors made with molecule I, devices made using the shorter molecule Co(tpy-SH)$_2$ (molecule II) often had an average conductance that was comparable to the conductance quantum ($2e^2/h \sim 77$ μS). In fact, we were sometimes able to observe the insertion of these high-conductance molecules into the gap between the electrodes during the electromigration process. In Fig. 3a, a large bias I–V curve taken during an electromigration process is shown. The current suddenly increased at approximately 0.9 V, indicating that one or more molecules became inserted to the gap between the electrodes. The low bias conductance of the device after this event (solid curve, Fig. 3b) was approximately five times larger than before the event (dotted curve, Fig. 3b). Moreover, a zero-bias peak in dI/dV was observed after the molecule insertion, which was not present before.

The peak in dI/dV is a generic feature of these devices and has been seen in more than 30 samples. The peak is due to the Kondo effect [13], which arises in a quantum-dot system with a non-zero spin, where electrons can tunnel coherently between the dot and the leads. This effect has been studied previously in semiconductor quantum dots [14,15]. There are two signatures of the Kondo effect. The first is that the zero-bias peak in dI/dV (the Kondo peak) decreases with increasing temperature and disappears around the Kondo temperature T_K. We observe this behavior in all our devices. Fig. 3c shows one device with the characteristic temperature dependence. T_K for this device is approximately 20 K. The second signature of the Kondo effect is its magnetic field dependence (Fig. 3d). In an applied magnetic field, the Kondo peak splits into two dI/dV peaks with a splitting of $\Delta V = 2g\mu_B H/e$. H is the magnetic field and m_B is the Bohr magnetron. In Fig. 3d, the splitting of the Kondo peak is clearly visible, and the g-factor measured from the splitting is 2.00 ± 0.04. We have observed the same g-factor in over 10 devices. It is also consistent with the g-factor measured in devices with the longer molecule I for 2+ charge state.

3.3. Intercage vibrations in C_{140} transistors

Finally, we made SETs with single molecules of C_{140} (molecule IV). I–V curves of one such SET at different V_g's are shown in Fig. 4a. An excited level (solid arrow) is seen in these curves. By the same analysis as explained in the Section 3.1, the energy of this level was measured to be approximately 11 meV.

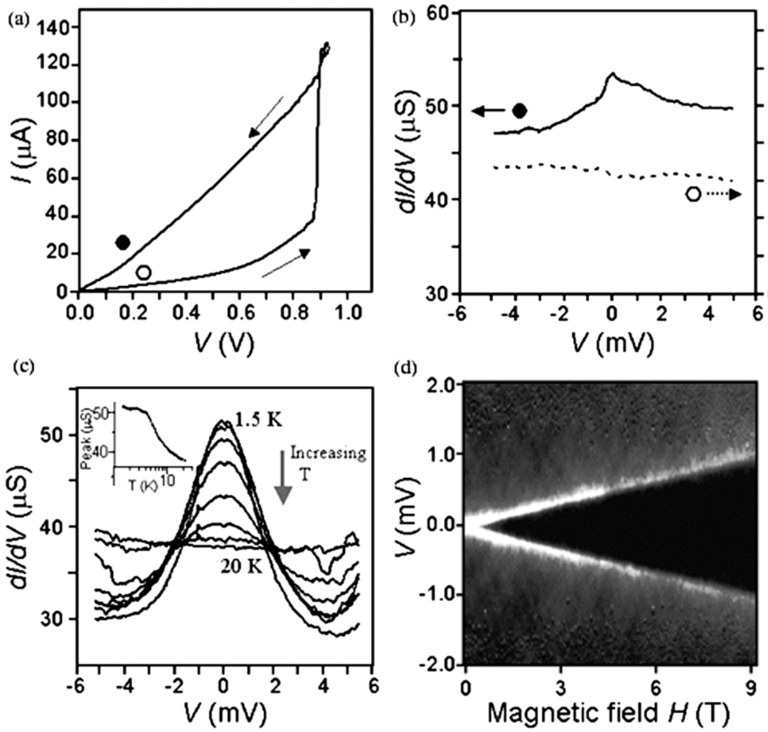

Fig. 3. The Kondo effect in single molecule transistors (molecule II). (a) A large bias I–V curve of a broken gold wire with adsorbed [Co(tpy-SH)$_2$]$^{2+}$ at 1.5 K. At approximately 0.9 V, the current level suddenly increases due to the incorporation of a molecule in the gap. (b) The low-bias conductance of the sample increases approximately five times after the incorporation of a molecule (solid line) and displays a peak at zero bias. (c) The temperature dependence of the Kondo peak for a device with molecule II. The inset shows the $V=0$ conductance as a function of temperature. The peak height decreases approximately logarithmically with temperature and vanishes at approximately 20 K. (d) Magnetic field dependence of the Kondo peak (bright lines). dI/dV is plotted as a function of V and H. The peak splitting varies linearly with magnetic field. These data were taken at the base temperature ($<$100 mK) of a dilution refrigerator.

More than half of C_{140} devices measured so far showed a level near 11 meV for both charge states and some of them show levels near multiples of 11 meV. These behaviors suggest that the 11 meV level in C_{140} SETs is most likely vibrational.

Calculations show that the six lowest vibrational modes of a single C_{140} molecule are 'intercage' modes where each C_{70} unit behaves like a single mass. These vibrational modes have also been seen experimentally by Raman spectroscopy [10]. In particular, it is known

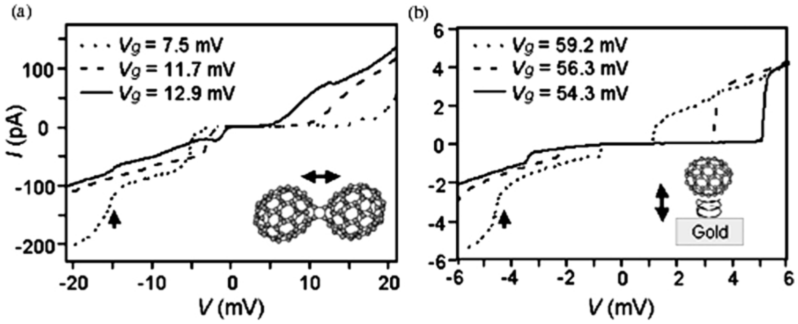

Fig. 4. Intercage vibrations in C_{140} transistors. (a) I–V curves measured from a C_{140} SET. They display Coulomb blockade, whose width changes with V_g. The arrow marks a current step near 15 mV, and it corresponds to a vibrational excitation with an energy near 11 meV. The schematic of this 11 meV intercage vibrational mode is shown in the inset. (b) I–V curves measured form a C_{70} SET. The arrow marks a current step corresponding to a 'bouncing-ball' mode (see the text) excitation with an energy near 3 meV.

that there is an intercage 'stretch' mode of C_{140} (schematically shown in the inset to Fig. 4a) that occurs at 11 meV. Therefore, we can make a direct correspondence between the observed 11 meV level and the stretch vibrational mode of C_{140}. Making such a correspondence was not possible for molecule I (Section 3.1) because of the larger number of low-energy normal modes. Our data also indicate that the 11 meV mode in C_{140} couples strongly to the motion of tunneling electrons, since the current increases significantly, when this level is accessible.

I–V curves of a device with C_{70} (molecule III) are also shown in Fig. 4b. They display Coulomb blockade and an excited level with an energy at 3 meV (arrow). However, no energy levels were seen in C_{70} devices near 11 meV, which confirms that the 11 meV level observed in C_{140} devices is indeed intrinsic to C_{140}. As in the case of C_{60} transistors [7], we attribute the level near 3 meV to the 'bouncing-ball' mode of C_{70} on the gold surface. The average energy of this level from several C_{70} devices is approximately 4 meV, which is consistent with a simple harmonic potential approximation for the van der Waals interaction between a C_{70} molecule and a gold surface.

4. Conclusions

We have fabricated a variety of single-molecule electronic transistors. In these devices, the vibrational modes of the molecule affect the electron transport properties significantly when the device resistance is high. We have also shown that it is possible to fabricate lower-resistance molecular devices with conductances comparable to the conductance quantum. Coherent electron transport occurs in such devices, and the Kondo effect is observed. These single-molecule transistors open up the possibility of chemically tailoring molecules in order to achieve designable transport properties.

Acknowledgments

We thank Eric Smith, Jason Petta, Markus Brink and Ji-Yong Park for help with measurements, and Mandar Deshmukh for discussions. We also thank professor Hoffmann and his research group members for their help with normal mode calculations. This work was supported by NSF, through individual-investigator grants, the Cornell Center for Materials Research, and the use of the National Nanofabrication Users Network. Support was also provided by the Packard Foundation and the US Department of Energy.

References

[1] A. Aviram, M.A. Ratner, Chem. Phys. Lett. 29 (1974) 277.

[2] L.A. Bumm, J.J. Arnold, M.T. Cygan, T.D. Dunbar, T.P. Burgin, L. Jones, D.L. Allara, J.M. Tour, P.S. Weiss, Science 271 (1996) 1705.

[3] X.D. Cui, A. Primak, X. Zarate, J. Tomfohr, O.F. Sankey, A.L. Moore, T.A. Moore, D. Gust, G. Harris, S.M. Lindsay, Science 294 (2001) 571.

[4] M.A. Reed, C. Zhou, C.J. Muller, T.P. Burgin, J.M. Tour, Science 278 (1997) 252.

[5] C. Kergueris, J.P. Bourgoin, S. Palacin, D. Esteve, C. Urbina, M. Magoga, C. Joachim, Phys. Rev. B 59 (1999) 12505.

[6] H. Park, A.K.L. Lim, J. Park, A.P. Alivisatos, P.L. McEuen, Appl. Phys. Lett. 75 (1999) 301.

[7] H. Park, J. Park, A.K.L. Lim, E.H. Anderson, A.P. Alivisatos, P.L. McEuen, Nature 407 (2000) 57.

[8] J. Park, A.N. Pasupathy, J.I. Goldsmith, C. Chang, Y. Yaish, J.R. Petta, M. Rinkoski, J.P. Sethna, H.D. Abruna, P.L. McEuen, D.C. Ralph, Nature 417 (2002) 722.

[9] M. Maskus, H.D. Abruna, Langmuir 12 (1996) 4455.

[10] S. Lebedkin, W.E. Hull, A. Soldatov, B. Renker, M.M. Kappes, J. Phys. Chem. B 104 (2000) 4101.

[11] H. Grabert, M.H. Devoret, Single Charge Tunneling: Coulomb Blockade Phenomena in Nanostructures, Plenum, New York, NY, 1992.

[12] H. Oshio, H. Spiering, V. Ksenofontov, F. Renz, P. Guetlich, Inorg. Chem. 40 (2001) 1143.

[13] E.L. Wolf, Principles of Electron Tunneling Spectroscopy, Oxford Univ. Press, Oxford, 1989, Ch. 8.

[14] D. Goldhaber-Gordon, H. Shtrikman, D. Mahalu, D. Abusch-Magder, U. Meirav, M.A. Kastner, Nature 391 (1998) 156.

[15] W.G. van der Wiel, S. De Franceschi, T. Fujisawa, J.M. Elzerman, S. Tarucha, L.P. Kouwenhoven, Science 289 (2000) 2105.